Original Article
ISSN (Online): 2454-1907

International Journal of Engineering Technologies and Management Research
October 2023 10(10), 1–19

DEVELOPMENT OF MULLITE- CARBON REFRACTORY CERAMIC COMPOSITE FROM LOCALLY SOURCED MATERIALS

Ifeyinwa Glory Ibekwe [1], Fatai Olufemi Aramide [1]

[1] Department of Metallurgical and Materials Engineering, Federal University of Technology P.M.B. 704, Akure, Nigeria

Received 25 August 2023
Accepted 26 September 2023
Published 10 October 2023

Corresponding Author

Ifeyinwa Glory Ibekwe,
gloryibekwe51@gmail.com

DOI
10.29121/ijetmr.v10.i10.2023.1366

Funding: This research received no specific grant from any funding agency in the public, commercial, or not-for-profit sectors.

ABSTRACT

In the pursuit of developing a mullite- carbon refractory ceramic composite with optimum physical and mechanical properties modified with additives, experimental studies were carried out using local materials from Nigeria's south-south and south-west regions. Kaolin clay was crushed to 2 mm and ball-milled into powder. Ground kaolin was homogeneously blended with graphite using a ball mill and sieved through a 300µm electric sieve. The homogeneous mix was combined with predetermined Magnesium Oxide proportions, compacted, and fired at 1300 °C, 1400 °C, and 1500 °C. Extensive tests followed, including X-ray diffraction (XRD) for phase analysis, ultra-high- resolution field emission scanning electron microscopy equipped with energy-dispersive spectroscopy (SEM-EDS) for microstructural morphology, and assessments of mechanical and physical properties. Findings indicated that additive inclusion spurred mullite phase development between 1300°C and 1500°C, enhancing their physico- mechanical properties. Among the samples, Sample R composed of 15% MgO, 65% kaolin, and 20% graphite, fired at 1500°C, displayed optimal physico-mechanical properties (95.8%) and favorable mullite formation (46.0%) was achieved.

Keywords: Mullite, Kaolin, Graphite, Magnesium Oxide, Sintered Samples, Ceramic Composition' Physico- Mechanical Properties

1. INTRODUCTION

The development of mullite-carbon refractory ceramic composites has been a subject of significant interest in materials science and engineering. Mullite, a mineral phase composed of alumina and silica (3Al2O3. 2SiO2) Lima et al. (2022), possesses excellent thermal stability, mechanical strength, and resistance to high temperatures. The incorporation of carbon additives into the mullite matrix offers additional benefits, such as improved mechanical properties and enhanced refractory characteristics Pooladvand et al. (2011). This composite material has found wide applications in various industries that require materials capable of withstanding extreme heat conditions Choo et al. (2019). It is particularly sought

after in industries such as metallurgy, glass manufacturing, and furnace linings, where elevated temperature resistance and mechanical strength are crucial Aramide (2015). Extensive research has confirmed that the incorporation of the mullite phase in ceramic composites enhances both their mechanical and refractory properties. This allows for potential optimization of properties in ceramic matrix composites. Numerous studies in the literature have provided evidence supporting the advantages of mullite development in composites. Olajide et al. (2020) focuses on investigating the chemical composition, phase transitions, and structural changes of mullite generated through the sintering naturally occurring kaolinite clay and the findings unveiled that a more pronounced mullite phase was achieved through heightened alumina content when subjected to the elevated temperature. Aramide & Akintunde (2017) explore the impact of silicon carbide on phase development in a mullite-carbon ceramic composite. The objective of the research was to examine the impact of introducing silicon carbide and varying sintering temperatures on the phase development within a ceramic composite composed of kaolin and graphite. Behera & Bhattacharyya (2020), conducted a study on the sintering and microstructural analysis of mullite, which was synthesized using kaolinite and reactive alumina with the addition of MgO and TiO2. The researchers examined the effect of these additives on phase creation, microstructural evolution, densification, and mechanical strength of the resulting mullite ceramic. Zhu & Yan (2017) studied the microstructures and traits of porous ceramics based on mullite, which were manufactured using coal ash with the inclusion of Al2O3. In this study, the authors utilized coal fly ash slurry samples enriched with varying amounts of Al2O3 to produce mullite-based porous ceramics. Vodova et al. (2014) conducted a study to investigate the influence of CaO inclusion on the mineralogical composition and mechanical properties of ceramic tiles. In the study, addition of additives in ceramic composite has a significant influence on the mineralogical composition of the fired body. Olanrewaju et al. (2019) conducted a study to examine the impact of MgO and Cr2O3 additives on mullite formation from locally sourced Nigerian kaolin-calcined alumina sintered compacts. The researchers synthesized mullite by sintering the kaolin-alumina mixture obtained from Nigeria and the results indicated successful synthesis of mullite, as evidenced by the dominant presence of mullite phases in the XRD patterns at 1600°C. Liu et al. (2022) evaluated the impact of adding Al(OH)3 on the densification mechanism and characteristics of reaction-sintered mullite-corundum composite ceramics. The study focused on examining the influence of sintering temperature and Al(OH)3 content on the phase composition, microstructure, and mechanical properties of the ceramics. The results revealed that as the temperature increased from 1480°C to 1560°C, the increased mullite content enhanced the mechanical properties of the composite ceramics. Aladesuyi et al. (2016) studied the phase and microstructural changes that took place during the firing process of a blend composed of 75% Nigerian kaolin and 25% calcinated alumina powder. The aim was to understand the progression of microstructure in a uniformly mixed combination of 75% weight of kaolinite clay powder sourced from Nigeria and 25% weight of finer grades of calcinated alumina powder (with an average particle size, d50, of 6-8 mμ). Based on the literature review, it was established that the sintering temperature significantly influences the physical and mechanical properties of the sintered samples. Increasing the sintering temperature has a positive impact on properties such as bulk density, strength, toughness, etc., thereby reducing the porosity in the sintered samples. Additionally, the addition of additives promotes the formation of Mullite, a desirable structure for refractory applications, which typically forms at high temperatures. In this research, the focus is on developing a mullite-carbon refractory ceramic composite using

locally sourced materials, namely raw kaolin, spent graphite, and the incorporation of additives (MgO).

The study aims to explore the effects of varying firing temperatures on the physico-mechanical properties of the composite, as well as the microstructural phases that develop within the samples.

2. MATERIALS AND METHODS

2.1. MATERIALS

Raw kaolin sample employed in this investigation was obtained from Okpella in Edo state Nigeria. Spent Graphite Electrode [SGE] in powdered form was obtained from chemical store (Pascal chemicals) Akure, Ondo state Nigeria. High Purity Oxides such as magnesium oxide and calcium oxide were obtained from Pascal chemicals store, Akure, Ondo state Nigeria.

2.2. METHODS

2.2.1. RAW CLAY PREPARATION

The kaolin was first crushed to about 2 mm and reduced to fine grains using ball mill. According to the composition shown in Table 1, the powdered samples of the ground kaolin and powdered graphite were thoroughly blended in a ball mill, the uniform sample was sifted through a 300μm sieve opening following to ASTM standards using an electric sieve shaker. The material that passed through the 300μm sieve was utilized in samples preparation.

2.2.2. PRODUCTION OF CERAMIC COMPOSITE SAMPLES

The samples containing a mixture of kaolin, graphite, and additive (MgO, CaO) were compacted using hydraulic press. The moulded samples were sintered at 1300 °C, 1400 °C,1500 °C and was held at the temperature for 6 hours in an electric furnace. The fired samples were subjected to different test such as physical test (apparent porosity, bulk density, water absorption) mechanical test (cold crushing strength, young modulus, absorbed energy).

2.2.3. PHASE AND MINERALOGICAL COMPOSITION OF PREPARED SAMPLE

The mineral phases within the sintered samples were subsequently characterized using X- ray diffractometry (XRD) analysis. Ultra- high resolution field emission scanning electron microscope (SEM) equipped with energy dispersive spectroscopy (EDS) was employed to investigate the microstructure of the samples.

2.3. EXPERIMENTAL PROCEDURE

Table 1

Table 1 The Composition of Various Ceramic Composite Samples Used for the Experimental Investigation.

Sample Designation	Composition of Ceramic
SAMPLE M	80% kaolinite + 20% graphite
SAMPLE P	75% kaolinite + 20% graphite + 5% MgO
SAMPLE Q	70% kaolinite + 20% graphite + 10% MgO
SAMPLE R	65% kaolinite + 20% graphite + 15% MgO

2.4. TESTING

2.4.1. PHYSICAL TESTS

1) Apparent porosity (AP)

Samples from each ceramic composite category underwent a drying procedure lasting several hours at a specific temperature. The weight of each dried sample was recorded and designated as "E." Subsequently, the samples were placed in water for a soaking period and measured while suspended in air, with this weight noted as "W." Lastly, the weight of each specimen was measured again while fully submerged in water. This was designated as Aramide et al. (2016).

The apparent porosity was determined using the formula:

$$p = \frac{(W-E)}{(W-S)} x\ 100\% \tag{2.1}$$

2) Bulk density (BD)

The test samples underwent a drying process to ensure complete removal of water. The weights of the samples in their dry state were measured and documented. Subsequently, after cooling, they were placed into a beaker filled with water, leading to the observation of bubbles as the pores within the specimens became saturated. The weights of the soaked samples were then measured and recorded. Following this, each sample was individually suspended in a beaker, sequentially using a sling, and the respective weights while suspended were measured and recorded. Aramide et al. (2016).

Bulk densities of the sample were determined using the formula below:

$$Bulk\ density = \frac{E}{(W-S)} \tag{2.2}$$

Here E denotes weight of dried specimen, S signifies weight of dried specimen suspended in water, and W stands for weight of soaked specimen suspended in air.

3) Water absorption

The test specimen was desiccated within an oven until a consistent weight of the specimen was achieved. Subsequently, the specimen was submerged in water within a container, ensuring it remained suspended without making contact with the container's base. The container was then gradually heated until the water reached a boiling point. Following the boiling process and subsequent recondensation of water vaporized, the specimen was permitted to cool to ambient temperature. Following cooling, specimen was carefully dried, blotted, and subsequently re- measured. Aramide et al. (2016).

The percentage water absorption was calculated as from:

$$\%\ \text{water absorption} = \frac{(\text{Soaked wt} - \text{dried wt})}{(\text{Dried wt})} \tag{2.3}$$

2.4.2. MECHANICAL PROPERTIES

Cold compression strength, young modulus, and absorbed energy

The purpose of the cold compression strength test was to assess the sample's resistance to compression until it reaches failure, providing insights into its potential behaviour under a force. The conventional ceramic specimens were dried using an oven at a specific temperature and subsequently cooled. The cold compression strength evaluations were executed utilizing an INSTRON 1195 machine with a consistent crosshead speed of 10mm per minute. The specimens were prepared following the guidelines of ASTM C133-97 (ASTM C133-97, 2003) for cold crushing strength according to Aramide et al. (2016). The calculations for cold crushing strength, modulus of elasticity, and absorbed energy were derived from the provided equation for both standard and conditioned samples.

$$CCS = \frac{(Load\ to\ fracture)}{(Surface\ area\ of\ sample)} \tag{2.4}$$

2.5. ANALYSIS

2.5.1. QUALITATIVE AND QUANTITATIVE XRD

The samples were prepared for XRD analysis using a back loading preparation technique as described by Kleeberg et al. (2008). They were examined using a Malvern Panalytical AERIS diffractometer equipped with a PIXcel detector and fixed slits, utilizing Fe-filtered Co-Kα radiation. The X'Pert Highscore plus software was employed for phase identification. The relative quantities of phases (weight %) were calculated using the Rietveld method.

2.5.2. SCANNING ELECTRON MICROSCOPY

Morphology and microanalysis of the composite samples were assessed using ultra- high resolution field emission scanning electron microscope (SEM) equipped with energy dispersive spectroscopy (EDS). Images of particles were captured using a secondary electron detector.

3. RESULTS AND DISCUSSIONS

3.1. EFFECT OF SINTERING TEMPERATURE ON THE MULLITE-CARBON CERAMIC COMPOSITES

3.1.1. EFFECT OF SINTERING TEMPERATURE ON THE PHASE DEVELOPMENT IN MULLITE-CARBON CERAMIC COMPOSITES WITHOUT ADDITIVES

Figure 1 and Figure 2 shows the XRD results of the phases developed in sintered Sample M (control). It was observed that the XRD of sintered sample contained some phases with their composition such as periclase, graphite, enstatite, mullite, gehlenite, forsterite, cristobalite, anorthite, anatase, cordierite and spinel. SEM/EDS micrographs at varied temperature (a) 1300 ℃ (b) 1400 ℃ (c) 1500 ℃ were presented in Figure 3 and the different elements (oxygen, aluminium, silicon, iron, titanium) present in the fired phase was shown. The XRD pattern in Figure 1 and Figure 2 presented that mullite, periclase and graphite were the major phases in the

sintered samples while other phases were observed at lower intensity. From the composition of the starting materials utilized in fabricating the sintered samples, it was shown that mullite was not among the starting materials. The XRD results obtained in Figure 1 presented that the mullite phase formed at 1300 °C was 29.1%. It is generally known that mullite phase was formed via solid state transformation of raw kaolin clay at high temperature above 1000 °C and this process is known as Mullitization process. Chargui et al. (2018), Abubakar et al. (2020), Soto et al. (2022).

$$3(Al_2O_3.\,2SiO_2.\,2H_2O) \rightarrow 3Al_2O_3.\,2SiO + 4SiO_2 + 6H_2O \quad (3.1)$$

As the sintering temperature was increased from 1300 °C to 1400 °C, it was observed that the mullite content reduced from 29.1% to 17.3% as shown in XRD result in Figure 1 and this was due to the increase in other phases been formed at 1400 °C (periclase, graphite, silica and anatase). As the sintering temperature was raised to 1500 °C, the mullite content increased largely to 34.9% from 17.3% been observed at 1400 °C. The further increment in mullite content was as a result of the appearance of kaolinite peak content which occurred when periclase, graphite, anatase and cristobalite peak reduced to a low intensity. Similar results have been evaluated by some authors Aramide & Akintunde (2017) and Chargui et al. (2018).

Figure 1

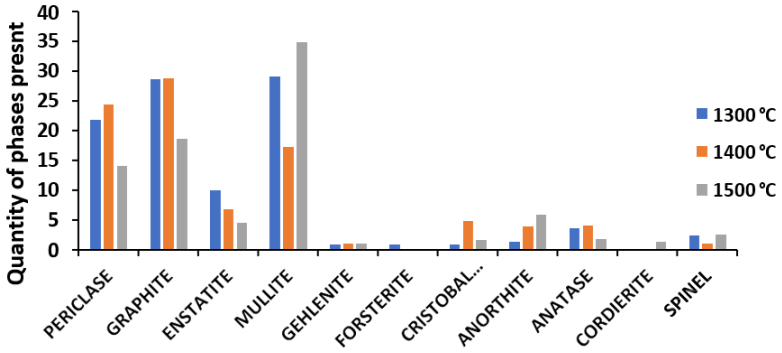

Figure 1 XRD Results of Sintered Sample M at Sintering Temperature of 1300 °C, 1400 °C and 1500 °C.

Figure 2

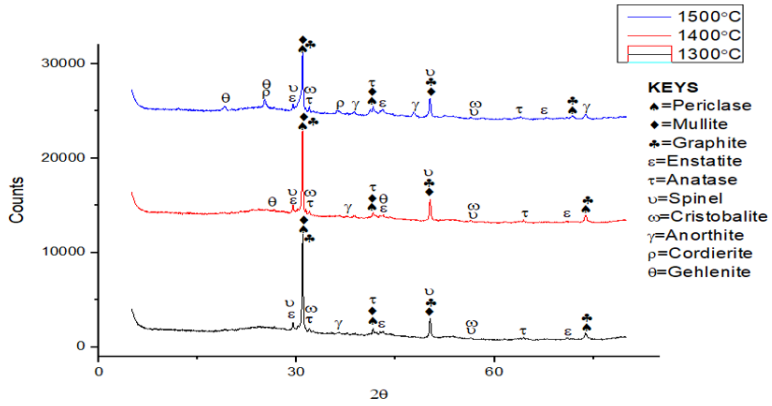

Figure 2 XRD Patterns of Sintered Control Sample M at Sintering Temperature of 1300 °C, 1400 °C and 1500 °C.

Figure 3

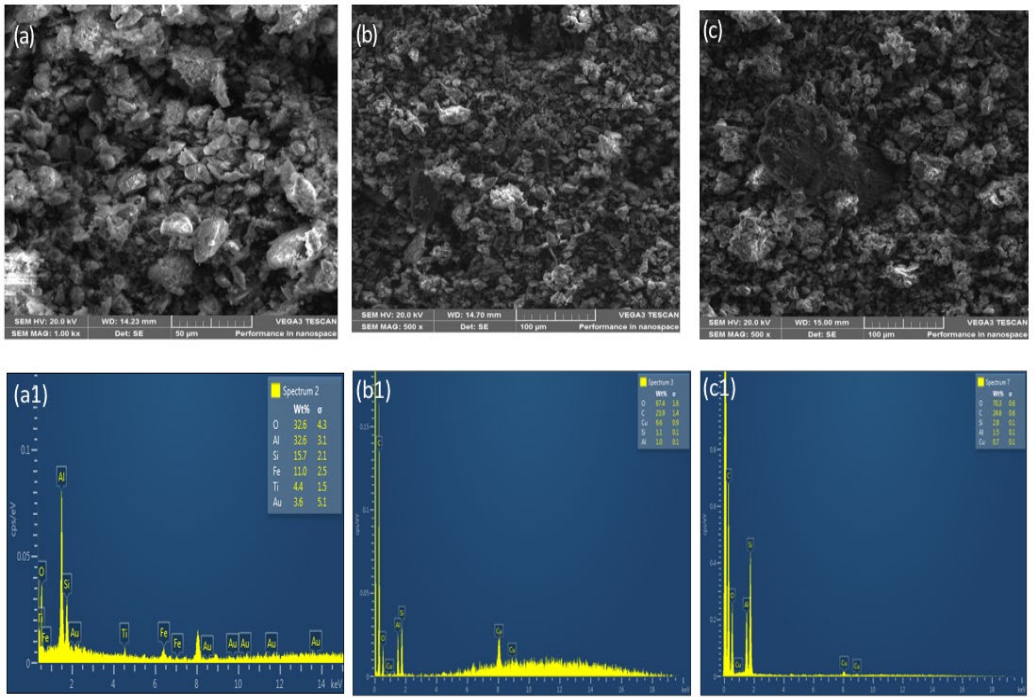

Figure 3 Showing SEM/EDS Micrographs of Control Sample M at Varied Temperatures: (a) 1300 °C, (b) 1400 °C (c) 1500 °C

3.1.2. EFFECT OF SINTERING TEMPERATURE ON THE PHASE DEVELOPMENT IN MULLITE-CARBON CERAMIC COMPOSITES WITH ADDITIVES

1) Effect of sintering temperature on the phase development in mullite-carbon ceramic composites with 5% MgO additives

Figure 6 shows that MgO present in the SEM/EDS result facilitated more formation of mullite phase in the sintered sample. It was observed in the XRD pattern given in Figure 4 and Figure 5 that as 5%MgO additive was introduced into the sintered sample, more mullite content was developed reaching 44.4% as compared to 29% formed at the control sample at sintering temperature of 1300°C. This was corroborated by the findings of Olanrewaju et al. (2019) and Choo et al. (2019), addition of chemical additive into the clay sample either accelerates or inhibits the growth of mullite phases in the sample but in the case of MgO additive, the formation of mullite was accelerated and both primary and secondary mullite was formed. As the sintering temperature was increased to 1400 °C, mullite content slightly reduced (31.9%) and this occurred due to increase in the phases of periclase, graphite and cristobalite phase in the sintered sample as presented in the XRD result shown in Figure 4. As the sintering temperature was increased to 1500 °C, the periclase, graphite and cristobalite phase formed at 1400 °C was reduced and this led to the further formation of mullite phase which was increased to 35% from the 31.9% formed at 1400 °C. As MgO additive has been added to the raw material, silica content decreased and complete mullitization was achieved at this stage at high intensity Tkaczewska (2015). Wei & He (2019).

Figure 4

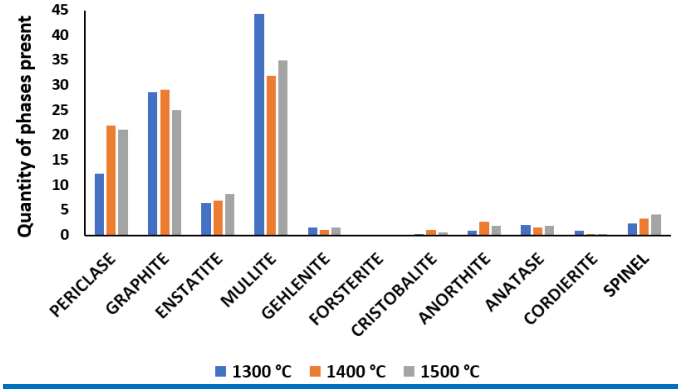

Figure 4 XRD Results of Sintered Sample P at Sintering Temperature of 1300 °C, 1400 °C and 1500 °C.

Figure 5

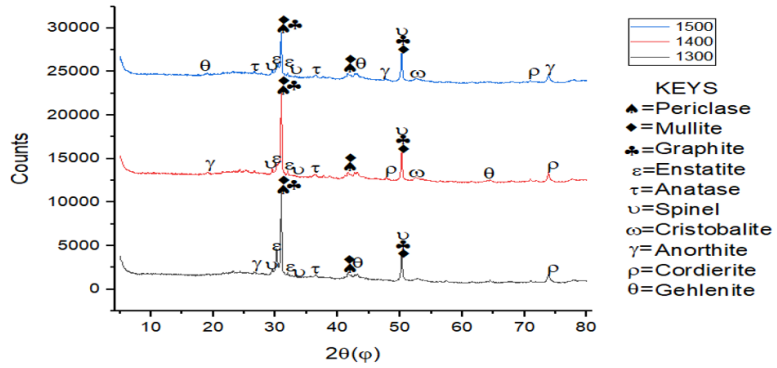

Figure 5 XRD Patterns of Sintered Sample P with 5% MgO Additive at Sintering Temperature of 1300 °C, 1400 °C and 1500 °C.

Figure 6

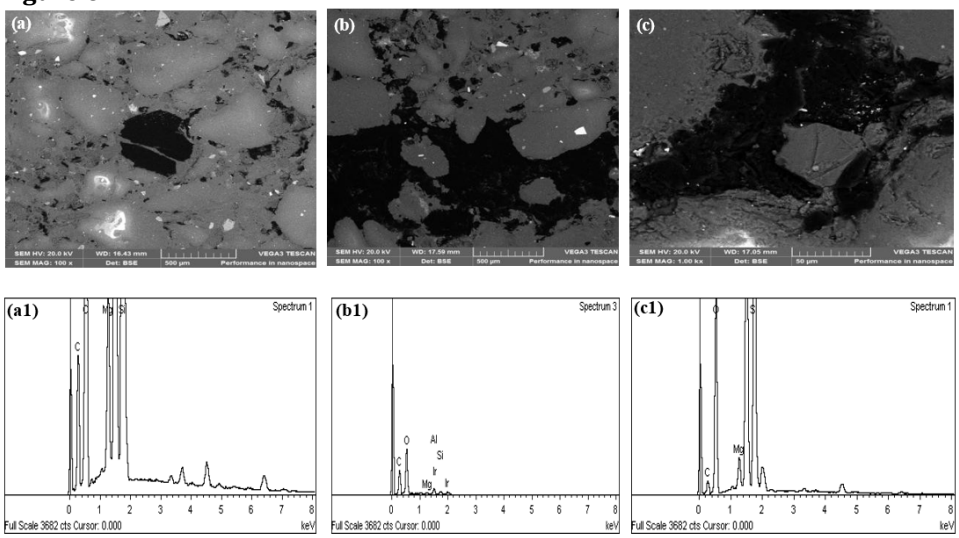

Figure 6 Showing SEM/EDS Micrographs of Sample P at Varied Temperatures: (a) 1300 °C, (b)1400 °C (c) 1500 °C

2) Effect of sintering temperature on the phase development in mullite-carbon ceramic composites with 10% MgO additives

As presented in XRD result in Figure 7 and Figure 8, it was observed for sample Q that mullite, graphite and periclase were formed at high intensity while other minerals were observed at low intensity. Mullite content achieved at sintering temperature of 1300 ℃ was 32.7% which was lower compared than 44.4% obtained in sample P. At sintering temperature of 1400 ℃, mullite content reduced slightly to 31.5% from 32.7% obtained at 1300 ℃, this reduction occurred due to the increase in periclase, and enstatite phases developed in the sintered sample. As the sample was fired at 1500 ℃, mullite content was reduced to 26.9%. The periclase content formed at sintering temperature of 1300 ℃ was 24.5% and as the firing temperature was raised to 1400 ℃, it increased to 25.9% from 24.5% gotten at 1300 ℃. As temperature was increased from 1400 ℃- 1500 ℃, the periclase content formed was 30.8% and this occurred due to the introduction of 10%MgO additive into the sintered sample. Graphite content decreased from 25.6% to 21.6% as temperature was increased from 1300 ℃- 1500 ℃. It was observed in the SEM/EDS result in Figure 9(a1) that the presence on Fe content reduced grain refinement in the microstructure of the sintered ceramic composite sample. According to Lecomte-Nana et al. (2013), firing sample which contain high Fe content at high sintering temperature accelerated the development of large mullite grains and the grains are separated widely from each other.

Figure 7

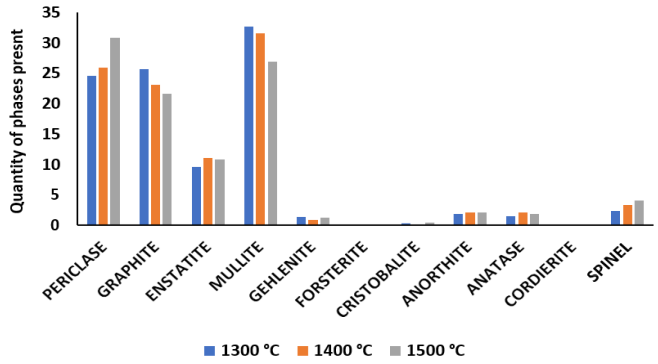

Figure 7 XRD Patterns of Sintered Sample Q with 10% MgO Additive at Sintering Temperature of 1300 ℃, 1400 ℃ and 1500 ℃.

Figure 8

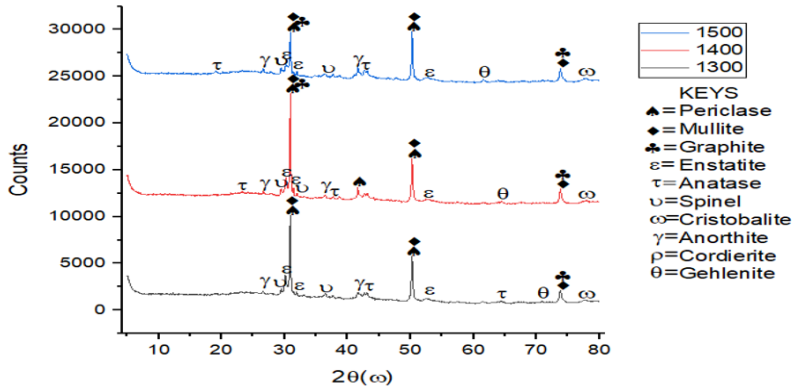

Figure 8 XRD Patterns of Sintered Sample Q with 10% MgO Additive at Sintering Temperature of 1300 ℃, 1400 ℃ and 1500 ℃.

Figure 9

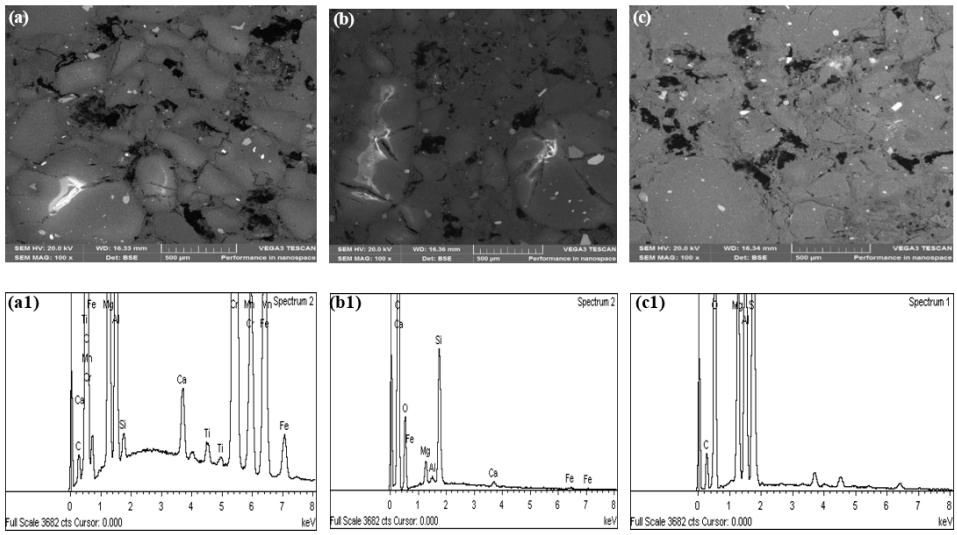

Figure 9 Showing SEM/EDS Micrographs of Sample Q at Varied Temperatures:
(a) 1300 °C, (b) 1400 °C (c) 1500 °C

3) Effect of sintering temperature on the phase development in mullite-carbon ceramic composites with 15% MgO additives

From the XRD pattern in Figure 10 and Figure 11, it was observed for sample Q that mullite, graphite and periclase were formed at high intensity while other minerals were observed at low intensity. Mullite content formed at sintering temperature of 1300 °C was 26.9%, it was observed that the microstructure of SEM/EDS result given in Figure 12(a1) showed a compacted sintered sample due to the presence of Aluminium content present in the sample which aids compaction. As the temperature was increased to 1400 °C, long separated grains of mullite were observed in the sintered sample the mullite phase formed increased to 36.1%. It was observed that at sintering temperature of 1500 °C, the EDS result given in Figure 12(c1) showed a well compacted sample and the mullite phase formed at this stage was 46% which is higher than those formed in previous sample. Mullite phases formation increased linearly with increase in sintering temperature while silica and graphite phases reduced linearly as the sintering temperature increased from 1300 °C to 1500 °C.

Figure 10

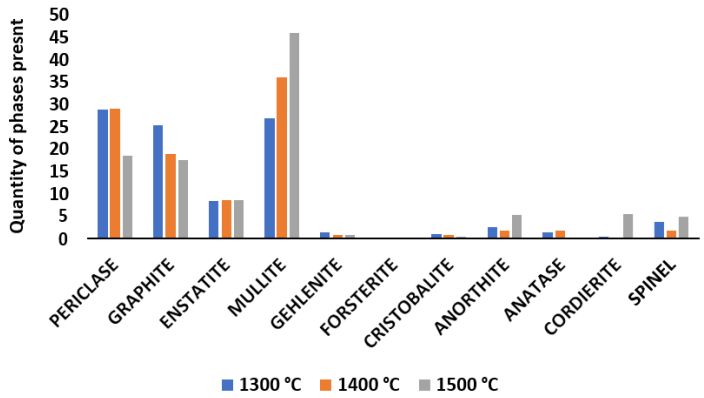

Figure 10 XRD Patterns of Sintered Sample R with 10% MgO Additive at Sintering Temperature of 1300 °C, 1400 °C and 1500 °C.

Figure 11

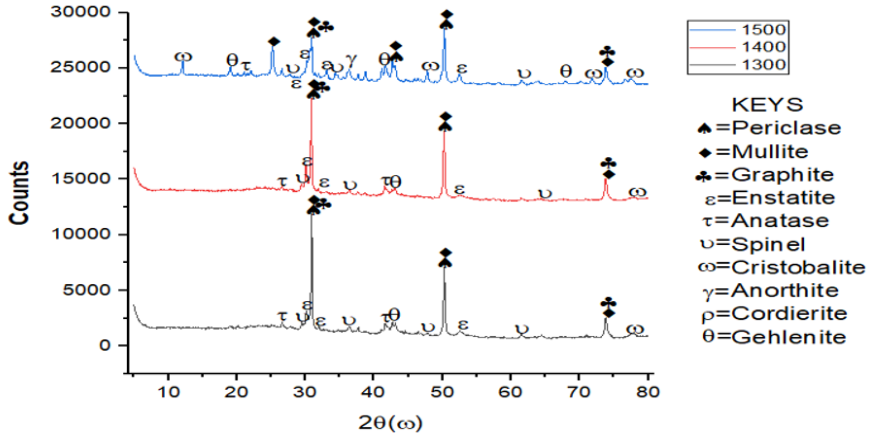

Figure 11 XRD Patterns of Sintered Sample R with 15% MgO Additive at Sintering Temperature of 1300 °C, 1400 °C and 1500 °C.

Figure 12

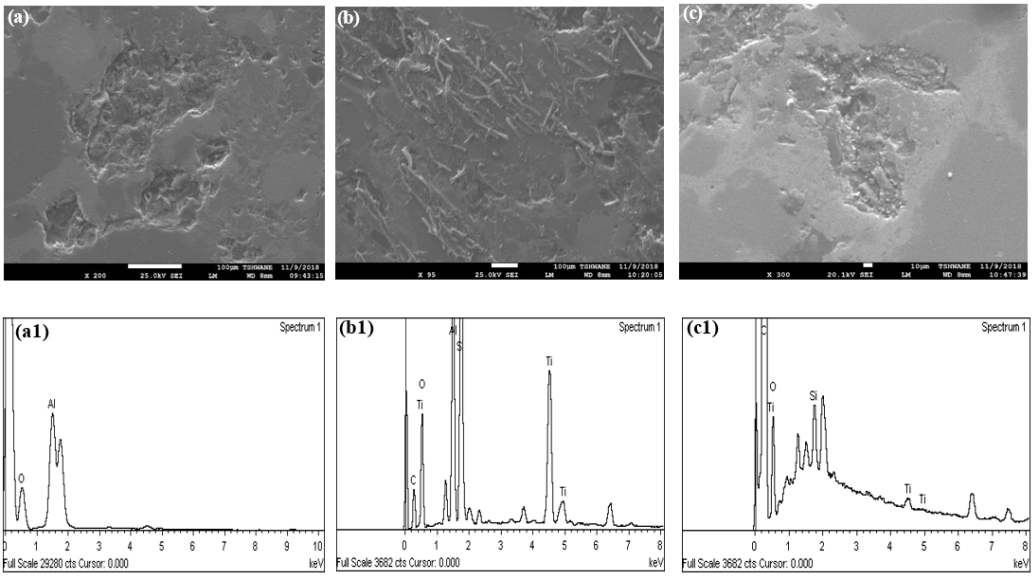

Figure 12 Showing SEM/EDS Micrographs of Sample R at Varied Temperatures: (a) 1300 °C, (b) 1400 °C (c) 1500 °C

3.2. EFFECT OF SINTERING TEMPERATURE ON THE PHYSICAL AND MECHANICAL PROPERTIES OF MULLITE- CARBON REFRACTORY CERAMIC COMPOSITE SAMPLES

3.2.1. EFFECT OF SINTERING TEMPERATURE ON THE PHYSICAL PROPERTIES OF SAMPLES WITH AND WITHOUT ADDITIVE AT DIFFERENT TEMPERATURE OF 1300 °C, 1400 °C AND 1500 °C.

The effect of sintering temperature on physical properties (apparent porosity, bulk density, and water absorption) of sample M (control), sample P (5% MgO), sample Q (10% MgO) and sample R (15% MgO) at different temperature of 1300 °C, 1400 °C and 1500 °C was presented in Table 2 and Figure 13 to Figure 15.

1) APPARENT POROSITY (AP)

Figure 13 and Table 2 shows that the AP of the control sample M sintered at 1300 °C was 21.33% and as sintering temperature increased to 1400 °C the AP reduced to 40.32%, this resulted to the densification of the sample as sintering temperature was increased from 1300 °C- 1400 °C as reviewed by Aramide et al. (2014), Brasileiro et al. (2006), the reduction in the value of AP from 1300 °C to 1400 °C was as a result of closing up some pores due to liquid state sintering. Firing the sintered sample at sintering temperature of 1500 °C led to the increase in the apparent porosity of the sample to 47.78%. The increment in AP from sintering temperature of 1400 °C- 1500 °C was due to carbon content present in the SEM/EDS result as reported in Figure 3. The carbon reacted with oxygen but due to the temperature at which the reaction took place, the carbon combusts leaving voids within the sintered sample. Similar work was carried out by Aramide et al. (2016). As presented in Figure 13 and Table 2 it was observed that the AP of the sintered sample P reduced to 26.36% when 5%MgO was added into sintered sample at sintering temperature of 1300 °C. as the temperature was raised to 1400 °C, AP reduced to 23.48% and at 1500 °C, it increased slightly to 23.53%. The AP of sample Q with 10%MgO additive reduced linearly from 25% to 17.93% with increase in sintering temperature from 1300 °C to 1500 °C while for sample R, the AP at 1300 °C was 19.93 and at 1400 °C, the obtained AP was 22.86% and as sintering temperature was increased to 1500 °C AP reduced to 17.00%. The filling up of intragranular voids created in the microstructure when varying content of MgO additive was added can be attributed to the reduction in AP as compared to that obtained in the control sample. Conclusively, AP reduces with addition of MgO additives.

Figure 13

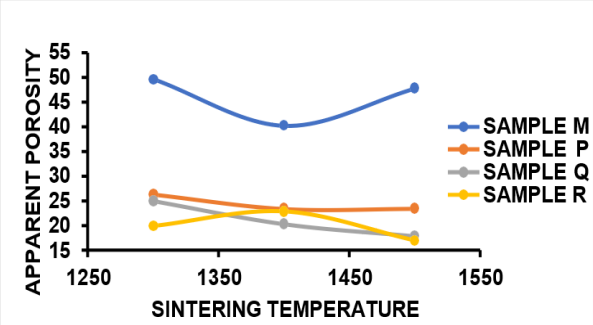

Figure 13 Effect of Sintering Temperature on AP of Sintered Samples M, P, Q, R.

2) BULK DENSITY (BD)

From Figure 14 and Table 2, it was observed that the BD of the control sample M sintered at 1300 °C was 1.9g/cm3 and as sintering temperature increased to 1400 °C the BD increased to 2.1g/cm3, while at sintering temperature of 1500 °C, it was reduced slightly to 2.0g/cm3. Compared to the BD value of the control sample M, better densification was achieved when MgO additive was added to the sintered sample. Sample P at sintering temperature of 1300 °C, BD value obtained was 2.21g/cm3, at 1400 °C it was increased to 2.23g/cm3 while at 1500 °C, there was a slight reduction in the BD of the sintered sample. Sample Q which contained 10% MgO additive, it was observed that the BD value increased linearly from 2.05g/cm3 to 3.24g/cm3 as sintering temperature increased from 1300 °C to 1500 °C. Sample

R at sintering temperature of 1300 °C has BD value of 3.13g/cm3, as sintering temperature was increased to 1400, the BD value reduced to 2.64g/cm3 but as the sintering temperature was increased to 1500 °C, the BD value increased to 3.68g/cm3. The densification of the sintered sample was due to the presence of Aluminium content present in the sample which aids compaction as shown in the SEM/EDS result given in Figure 12(a1). BD is inversely proportional to AP. Therefore, bulk density reduces with increase in porosity of the sample and the formation of open pores directly lowered some properties of bricks such as bulk density, strength, and corrosion resistance.

Figure 14

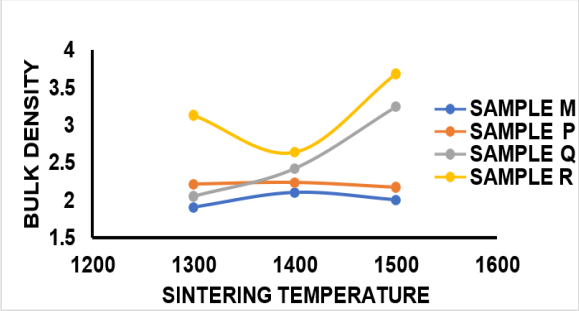

Figure 14 Effect of Sintering Temperature on BD of Sintered Samples M, P, Q, R.

3) WATER ABSORPTION (WA)

Table 2 and Figure 15 shows WA values which exhibited a consistent pattern aligned with the trend observed for apparent porosity, this implied that water absorption of the fired sample is directly proportional to the apparent porosity of the sample. Water absorption increased with increase in Porosity. Higher Water absorption reduced the strength of refractory. It was observed in Table 2 that water absorption increased linearly with increase in apparent porosity and Presence of voids gave room for water absorption in the sample.

Compared to the values obtained for sample M (control) without additive, it was observed that the samples with additives (P, Q and R) had low water absorption value and they were less porous compared to the WA value obtained in sample M. Hence, mullite formation was enhanced in samples with additives and therefore, the densification of the sintered ceramic composite was improved. As agreed with Karhu et al. (2020), the bulk density and porosity values are commonly utilized to determine suitable refractories for specific applications. Generally, higher density corresponds to lower porosity, and various properties, including strength, tend to be associated with the density and porosity levels.

Figure 15

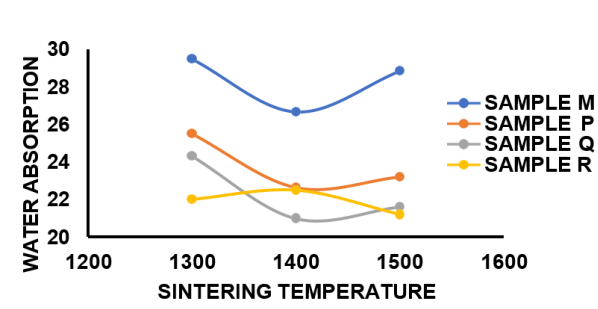

Figure 15 Effect of Sintering Temperature on WA of Sintered Samples M, P, Q, R.

3.2.2. EFFECT OF SINTERING TEMPERATURE ON THE MECHANICAL PROPERTIES OF SAMPLES WITH AND WITHOUT ADDITIVE AT DIFFERENT TEMPERATURE OF 1300 °C, 1400 °C AND 1500 °C

The effect of sintering temperature on mechanical properties (cold crushing strength, young modulus, and absorbed energy) of sample M (control), sample P (5% MgO), sample Q (10% MgO) and sample R (15% MgO) at different temperature of 1300 °C, 1400 °C and 1500 °C was presented in Table 2 and Figure 16, Figure 17, Figure 18

1) COLD CRUSHING STRENGTH (CCS)

From Figure 16 and Table 2, it was observed that the CCS of the control sample M at sintering temperature of 1300 °C was 4.16N/mm2, as the sintering temperature was increased to 1400 °C, CCS value increased to 6.65N/mm2 but at 1500 °C, the CCS value reduced slightly to 6.08N/mm2. The CCS value obtained for Sample P increased from 8.06N/mm2 to 8.72N/mm2 and as sintering temperature was increased to 1500 °C, the CCS obtained reduced to 7.28N/mm2. The CCS value obtained for Sample Q increased from 7.01N/mm2 to 9.1N/mm2 as the sintering temperature was increased from 1300 °C to 1500 °C while the CCS of Sample R which contained 15%MgO additive had 7.83N/mm2 at 1300 °C, 7.79N/mm2 at 1400 °C and was increased to 9.39N/mm2 as sintering temperature was raised to 1500 °C. It was observed that relationship also exists between the cold crushing strength and bulk density of a sintered sample; an increase in the bulk density of the sample, simply means that the sample contains more matter to bear the applied load, and this enhances the strength of the material. Similar study has shown that cold crushing strength increased as bulk density also increased; this trend therefore reduced the porosity of the sample Czechowski et al. (2015).

Figure 16

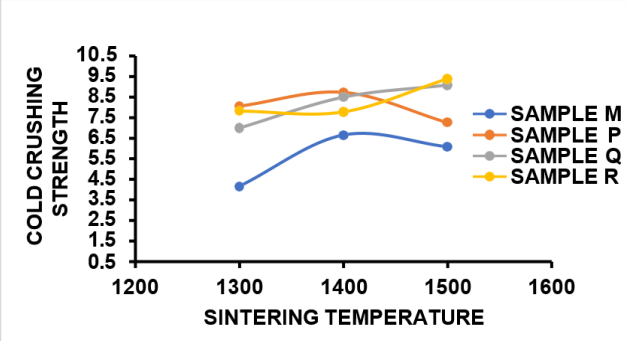

Figure 16 Effect of Sintering Temperature on CCS of Sintered Samples M, P, Q, R.

2) YOUNG MODULUS (YS)

Figure 17 shows that the variation of the young modulus with increased sintering temperature followed the same pattern with that observed for the cold crushing strength discussed earlier. Material with high young modulus possess higher hardness which is a major property of ceramic and can withstand high stress without permanent deformation. It was observed that sample M at sintering temperature of 1300 °C, the YM obtained was 4.16N/mm2, at 1400 °C, YM obtained was 6.63N/mm2 and at sintering temperature of 1500 °C, 6.09N/mm2 was achieved. The YM for sample P which contained 5%MgO additive at sintering

temperature of 1300 °C was 8.05N/mm2, at 1400 °C was 8.71N/mm2 and as it was fired at 1500 °C, the YM was 7.27N/mm2. Sample Q which contained 10%MgO additive at sintering temperature of 1300 °C had YM value of 7.01N/mm2, at 1400 °C was 8.41N/mm2 and at sintering temperature of 1500 °C was 8.69N/mm2. Sample R at sintering temperature of 1300 °C had YM value of 7.81N/mm2, at sintering temperature of 1400 °C was 6.78N/mm2 and as the sample was fired to 1500 °C, the YM value recorded was 9.38N/mm2.

Figure 17

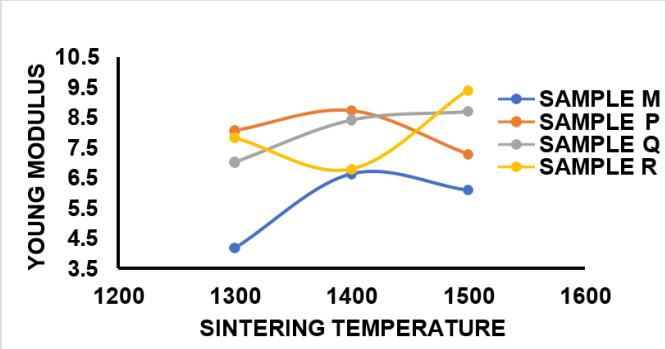

Figure 17 Effect of Sintering Temperature on YM of Sintered Samples M, P, Q, R.

3) ABSORBED ENERGY (AE)

As presented in Figure 18 and Table 2, it was observed that the AE of the control sample M at sintering temperature of 1300 °C was 5.96J, at sintering temperature of 1400 °C, the AE obtained was 6.8J, when the firing temperature was increased to 1500 °C, AE value of 5.58J was achieved. At 5%MgO additive for sample P at sintering temperature of 1300 °C, the energy absorbed was 7.21J, at 1400 °C was 8.82J and as the sintering temperature increased to 1500 °C, AE value was reduced to 7.06%. At 10%MgO additive for sample Q, it was observed that AE increased linearly from 7.05J to 8.2J as sintering temperature increased from 1300 °C to 1500 °C. sample R which contained 15%MgO. It was observed that at sintering temperature of 1300 °C, AE value achieved was 9.28J, as the sintering temperature increased to 1400 °C, the energy absorbed by the system was 7.8J and at temperature of 1500 °C, the AE value achieved was 8.60J. However, the overall observation was that ceramic composite samples which contained varying content of MgO additive absorbed more energy into the system compared to control sample which contained 0% additive.

Figure 18

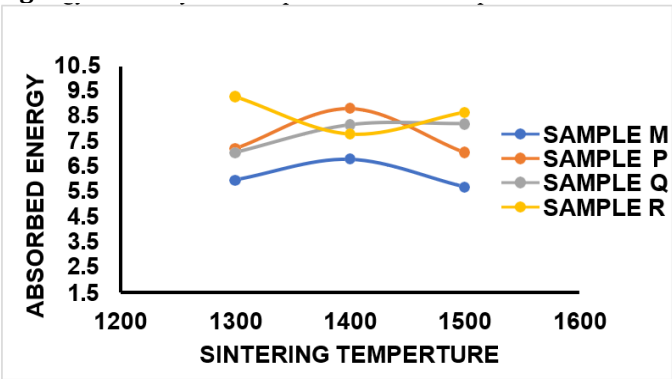

Figure 18 Effect of Sintering Temperature on AE of Sintered Samples M, P, Q, R.

3.3. DETERMINATION OF OPTIMUM PHYSICO- MECHANICAL PROPERTY

Table 2 and Table 3 displayed the outcomes of comparing physico-mechanical properties using a numerical index table, as outlined by Aramide et al. (2014). Within the table, numerical indicators were used to represent the relative values of the assessed properties on a scale of preference ranging from 1 to 12 (please refer to the key provided in Table 2 and Table 3). These numerical indices aid in identifying the optimal parameter for the development of mullite-carbon refractory ceramic composites.

Among the evaluated properties, apparent porosity and water absorption were categorized as "negative parameters," where the lowest value is considered ideal. Conversely, bulk density, cold crushing strength (CCS), young's modulus, and absorbed energy were classified as positive parameters, with the highest value being deemed optimal. Based on the data presented in Table 2, it is evident that sample R at sintering temperature of 1500°C had the optimum conditions with average points of 95.8%.

Table 2

Table 2 Key to Table 3.1

12	11	10	9	8	7	6	5	4	3	2	1
Excellent	Very Good	Good	Good	Good	Fair	Average	Below Average	Below Average	Poor	Poor	Poor

Table 3

Table 3 Numerical Index Table for the Evaluated Properties

	Sample M			Sample P			Sample Q			Sample R		
	1300	1400	1500	1300	1400	1500	1300	1400	1500	1300	1400	1500
Apppparent porosity (%)	49.63 12th (1)	40.32 10th(3)	47.78 11th(2)	26.36 9th (4)	23.48 6th (7)	23.53 7th (6)	25.00 8th (5)	20.36 4th (9)	17.93 2nd(11)	19.93 3rd(10)	22.86 5th (8)	17.00 1st (12)
Bulk density (g/cm³)	1.9 12th(1)	2.1 9th (4)	2.0 11th(2)	2.21 7th (6)	2.23 6th (7)	2.17 8th (5)	2.05 10th(3)	2.42 5th (8)	3.24 2nd(11)	3.13 3rd(10)	2.64 4th (9)	3.68 1st (12)
Water absorption (%)	29.51 12th(1)	26.67 10th(3)	28.86 11th(2)	25.51 9th (4)	22.64 6th (7)	23.21 7th (6)	24.32 8th (5)	21.00 1st (12)	21.62 3rd (10)	22.01 4th (9)	22.50 5th (8)	21.21 2nd(11)
CCS (N/mm²)	4.17 12th(1)	6.65 10th(3)	6.08 11th(2)	8.06 5th(8)	8.72 3rd(10)	7.28 8th (5)	7.01 9th(4)	8.51 4th(9)	9.1 2nd(11)	7.83 6th(7)	7.79 7th(6)	9.39 1st(12)
Young modulus(N/mm²)	4.16 12th(1)	6.63 10th(3)	6.09 11th(2)	8.05 5th(8)	8.71 2nd(11)	7.27 7th(6)	7.01 8th(5)	8.41 4th(9)	8.69 3rd(10)	7.81 6th(7)	6.78 9th(4)	9.38 1st(12)
Absorbed energy (J)	5.96 11th(2)	6.8 10th(3)	5.68 12th(1)	7.21 7th(6)	8.82 2nd(11)	7.06 8th(5)	7.05 9th(4)	8.15 5th(8)	8.2 4th(9)	9.28 1st(12)	7.8 6th(7)	8.66 3rd(10)

Total points/ 72	7	19	11	36	53	33	26	55	62	55	42	69
Average points/ 100	9.7	26.3	15.2	50	73.6	45.8	36.1	76.3	86.1	76.3	58.3	95.8
Remarks	Poor	Poor	Poor	Average	Good	Below Average	Below Average	Good	Very Good	Good	Fair	Excellent

4. CONCLUSION

Based on the findings of this study, it could be concluded that:

1) Sample M (control sample without additive) does not have the best mullite formation even with the rise in firing temperature from 1300 °C- 1500 °C. The mullite content formed was low compared to other sintered samples that contained additives. Also, poor densification/compaction was achieved within its microstructure, and this triggered the formation of pores within the sintered ceramic composite sample. The least value of bulk density, strength, young modulus, and absorbed energy was achieved in sample M. Also, the highest Apparent porosity value and water absorption value were achieved in this sample. Thus, sample M will not make a good material for refractory, and it would eventually cause catastrophic effects and would fail when used for high temperature application.
2) Sample R which contains 15%MgO additive, 65% kaolin, 20% graphite, fired at 1500 °C with optimum physico-mechanical properties of 95.8% has proven to be more effective in the formation of mullite with mullite content of 46.0.

CONFLICT OF INTERESTS

None.

ACKNOWLEDGMENTS

None.

REFERENCES

Abubakar, M., Muthuraja, A., Rajak, D., Ahmad, N., Pruncu, C., Lamberti, L., & Kumar, A. (2020). Influence of Firing Temperature on the Physical, Thermal and Microstructural Properties of Kankara Kaolin Clay : A Preliminary Investigation. Materials (Basel), 13(8). https://doi.org/10.3390/ma13081872.

Aladesuyi, O., Pal, M., Emetere, M., Das, S., & Oluseyi, A. (2016). Phase and Microstructural Evolution During Sintering of Mixture of 75 : 25 Nigeria Kaolin and Calcined Alumina Powder Compacts. Journal of Material and Environmental Sciences, 8(8), 2682-2838.

Aramide, F. O. (2015). Effects of Sintering Temperature on the Phase Developments and Mechanical Properties Ifon Clay. Leonardo Journal of Sciences, (26), 67-82.

Aramide, F. O., & Akintunde, I. B. (2017). Effect of Silicon Carbide on Phase Development in a Mullite-Carbon Ceramic Composite. Journal of Practices and Technologies, (31), 45-58.

Aramide, F. O., Akintunde, I. B., & Oyetunji, A. (2016). Insitu Synthesis and Characterization of Mullite-Carbon Refractory Ceramic Composite from Okpella Kaolin and Graphite. Usak University Journal of Material Sciences, 39 (1), 25-42. https://doi.org/10.12748/uujms.2017.39.

Aramide, F. O., Alaneme, K. K., Olumbambi, P. A., & Borode, J. O. (2014). Effects of 0.2Y- 9.8ZrO2 Addition on the Mechanical Properties and Phase Development of Sintered Ceramic Produced from Ipetumodu Clay. Faculty of Engineering Hunedoara. International Journal of Engineering, 7(4), 343-353.

Aramide, F. O., Alaneme, K. K., Olumbambi, P. A., & Borode, J. O. (2014). High Temperature Synthesis of Zirconia- Mullite- Zirconia Refractory Ceramic Composite from Clay Based Materials in Volume 5- Composite, Ceramic, Quasi- Crystals, Nanomaterials and Coating. Sustainable Industrial Processing Summit and Exhibition/ Shechtman International Symposium, 5, 155-17.

Behera, S. P., & Bhattacharyya, S. (2020). Sintering and Microstructural Study of Mullite Prepared from Kaolinite and Reactive Alumina : Effect of MgO and TiO2. International Journal of Applied Ceramic Technology. 18(17), 81- 90. https://doi.org/10.1111/ijac.13637.

Brasileiro, M. I., Oliveira, D. H. S., Lira, H. L., de Lima Santana, L. N., Neves, G. A., Novaes, A. P., & Sasak, J. M. (2006). Mullite Preparation from Kaolin Residue. In Materials Science Forum. Trans Tech Publications, Ltd., 530–531, 625–630. https://doi.org/10.4028/www.scientific.net/msf.530-531.625.

Chargui, F., Hamidouche, M., Belhouchet, H., Jorand, Y., Doufnoune, R., & Fantozzi G. (2018). Mullite Fabrication from Natural Kaolin and Aluminium Slag. Boletín de La Sociedad Española de Cerámica y Vidrio, 57(4), 169-177. https://doi.org/10.1016/j.bsecv.2018.01.001.

Choo, T. F., Salleh, A., Kok, K.Y., & Matori, K. A (2019). A Review on Synthesis of Mullite Ceramics from Industrial Wastes. Recycling, 4(3), 39. https://doi.org/10.3390/recycling4030039.

Czechowski, J., Podwórny, J., Gerle, A., & Dahlem, E. (2015). Investigating the Factors that Influence the Cold Crushing Strength of Shaped Refractories. Institute of Ceramics and Building Materials, Refractory Materials Division.

Karhu, M., Talling, B., Piotrowska, P., Adams, A., Sengottuvelan, A., Huttunen-Saarivirta, E., Boccaccini, A. And Lintunen, P. (2020). Ferrochrome Slag Feasibility as a Raw Material in Refractories: Evaluation of Thermo-physical and High Temperature Mechanical Properties. Waste and Biomass Valorization, 11, 7147- 7157. https://doi.org/10.1007/s12649-020-01092-4.

Kleeberg, R., Moneeke, T., & Hillier, S. (2008). Preferred Orientation of Mineral Grains in Sample Mounts for Quantitative XRD Measurements: How Random are Powder Samples? Clays and Clay Minerals, 56(4), 404-415. https://doi.org/10.1346/CCMN.2008.0560402.

Lecomte-Nana, G., Bonnet, J., & Soro, N., (2013). Influence of Iron on the Occurrence of Primary Mullite in Kaolin-Based Materials : A Semi-Quantitative X-Ray Diffraction Study. Journal of the European Ceramic Society, 33, 669-677. https://doi.org/10.1016/j.jeurceramsoc.2012.10.033.

Lima, L. K. S., Silva, K. R., Menezes, R. R., Santana, L. N. L., Lira, H. L. (2022). Microstructural Characteristics, Properties, Synthesis and Applications of

Mullite: A Review. Cerâmica, 68(385), 126-142. https://doi.org/10.1590/0366-69132022683853184.

Liu, Z., Xie, N., Zhang, H., Huang, S., Wu, C., He, S., Zhu, J., & Liu, Y. (2022). Effect of Al (OH)3 Addition on Densification Mechanism and Properties of Reaction-Sintered Mullite-Corundum Composite Ceramics. Journal of Asian Ceramic Societies, 10, 1-10. https://doi.org/10.1080/21870764.2022.2114145.

Olajide, S. T., Seun, S. O., Olanireti, E. I., & Olaleye, T. S. (2020). Chemical, Phase and Structural Change of Mullite Synthesized During Sintering of Kaolin. International Journal of Applied Ceramic Technology, 17(5), 2259-2264. https://doi.org/10.1111/ijac.13566.

Olanrewaju, A., Ajanaku, O., & Swapan, D. (2019). The Effect of MgO and Cr2O3 on Mullite Formation from Nigeria Sourced Kaolin-Calcined Alumina Sintered Compacts. IOP Conference Series : Materials Science and Engineering, 509. https://doi.org/10.1088/1757-899X/509/1/012007.

Pooladvand, H., Baghshahi, S., Mirhadi, B., Souri, A. R., & Arabi, H. (2011). Effect of MgO and CaO on Transformation of Andalusite to Mullite. Journal of Material Engineering and Performance, 21, 1637-1644. https://doi.org/10.1007/s11665-011-0071-5.

Soto, S. P., Eliche-Quesada, D., Martínez- Martínez, S., Pérez-Villarejo, L., & Garzón, E. (2022). Study of a Waste Kaolin as Raw Material for Mullite Ceramics and Mullite Refractories by Reaction Sintering, Materials, 15, 583. https://doi.org/10.3390/ma15020583.

Tkaczewska, E. (2015). Mullite from High Temperature Chemical Reaction Method - Evaluation of Stoichiometric A2o3/Sio2 Ratio, Phase Composition and Microstructure. International Journal of Scientific Research, 4(6), 137-140. https://www.doi.org/10.36106/ijsr.

Vodova, L., Sokolar, R., & Hroudova, J. (2014). The Effect of CaO Additives on the Mineralogical Composition and Mechanical Properties of Ceramic Tiles. International Scholarly and Scientific Research & Innovation 8(6), 717-720.

Wei, D., & He, H.-Y. (2019). High Strength Glass-Ceramics Sintered with Coal Gangue as a Raw Material. Science of Sintering, 51, 285-294. https://doi.org/10.2298/SOS1903285W.

Zhu, J. B., & Yan, H. (2017). Microstructure and Properties of Mullite-Based Porous Ceramics Produced from Coal Fly Ash with Added Al2O3. International Journal of Minerals and Metallurgical Materials, 24, 309-315. https://doi.org/10.1007/s12613-017-1409-2.